Chapter 17
Frequency Modulation (FM) Mode in Dynamic Atomic Force Microscopy—Non-contact Atomic Force Microscopy

In Chap. 15 we introduced the intermittent contact mode (tapping mode), which is a very successful operation mode in dynamic atomic force microscopy. Since this mode has so many advantages, why should we use any other mode? In this chapter we introduce the FM detection scheme (often named non-contact atomic force microscopy) which in some cases has advantages over the tapping mode: (a) The FM detection scheme can be used with high Q cantilevers ($Q > 1{,}000$, occurring in vacuum). For high Q cantilevers the tapping mode results in unacceptably long scanning times. (b) The inelastic dissipation in the tip-sample interaction can be easily measured during scanning. (c) From the measured data the tip-sample force can be obtained as a function of the distance.

In the FM detection scheme of AFM the cantilever does not oscillate at a fixed driving frequency (as in the tapping mode), but always oscillates at resonance. If the resonance frequency shifts due to a tip-sample interaction, the cantilever oscillation frequency follows this shift. In the FM mode, the amplitudes are so large that the tip-sample force cannot be approximated as linear. The frequency shift in the FM mode is proportional to a weighted average of the tip-sample force over a cantilever oscillation cycle. For large amplitudes, the frequency shift depends almost exclusively on the tip-sample interaction at the lower turnaround point. We will describe in detail the experimental setup and the different FM detection modes and compare the FM and AM detection modes. The time response in FM detection is not limited for high quality factors, as it is the case in AM detection. Therefore, the FM detection scheme can be used for cantilevers with high quality factors, i.e. in vacuum.

17.1 Principles of Dynamic Atomic Force Microscopy II

In Chap. 14, we derived the frequency shift in the limit of small oscillation amplitudes, i.e. the force was described as linear with the tip-sample distance in the range of the oscillation amplitude. In this limit, the frequency shift is proportional to the force gradient. However, for most cases of larger oscillation amplitudes or short-range

B. Voigtländer, *Scanning Probe Microscopy*,
NanoScience and Technology, DOI 10.1007/978-3-662-45240-0_17

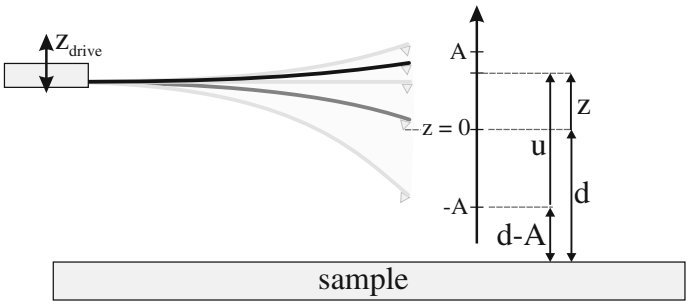

Fig. 17.1 Scheme of the cantilever vibration illustrating the corresponding coordinates

forces this limit does not hold at all. The interaction between tip and sample changes strongly on the scale of the vibrational amplitude of the cantilever.

In the following, we will consider a driven damped harmonic oscillator under the influence of a non-linear tip-sample force $F_{\mathrm{ts}}(d+z)$. The driving force is given by an external sinusoidal oscillation $z_{\mathrm{drive}} = A_{\mathrm{drive}} \cos(\omega t)$ of the cantilever base. This driving oscillation corresponds to a force $F_{\mathrm{drive}} = k z_{\mathrm{drive}}$. In FM detection, the driving at ω_{drive} is always applied at the actual resonance frequency[1] ω_0', which we call ω in the following, i.e. $\omega = \omega_{\mathrm{drive}} = \omega_0'$. The equation of motion for the driven damped harmonic oscillator with an external tip-sample force $F_{\mathrm{ts}}(d+z)$ added is written according to (2.17) as

$$m\ddot{z} + \frac{m\omega_0}{Q_{\mathrm{cant}}}\dot{z} + k(z - z_{\mathrm{drive}} - \Delta L) = F_{\mathrm{ts}}(d+z). \tag{17.1}$$

The relevant coordinates are indicated in Fig. 17.1. The zero point for z ($z = 0$) is given by the condition that the tip-sample force is compensated by the static cantilever bending ΔL, cf. Fig. 14.1 and (14.3). In this case the tip-sample distance is d.

In spite of the fact that a non-linear tip-sample force is included into the equation of motion, we approximate the solution $z(t)$ by a harmonic oscillation $z(t) = A\cos(\omega t + \phi)$. Since the oscillation in FM mode is always at resonance, $\phi = -90°$ and thus $z(t) = A\sin(\omega t)$. We will not solve the equation of motion (17.1), however, we will calculate the shift of the resonance frequency. The relation between tip-sample force and frequency shift Δf is more complicated than the simple proportional relation between Δf and the force gradient obtained in the small amplitude limit (14.7). For the case of the non-linear tip-sample force, the final result will be that the frequency shift corresponds to a properly weighted average of the tip-sample force over an oscillation period.

An expression for the frequency shift can be derived if we insert the explicit expressions for the harmonic oscillation of the cantilever $z(t)$ and its derivatives as

[1] Under the influence of the tip-sample force the resonance frequency of the free cantilever, ω_0, shifts to ω_0'.

well as the expression for ω_{drive} into (17.1). Subsequently we multiply (17.1) by $z(t) = A\sin\omega t$ and integrate over one period resulting in the following expression

$$-\int_0^T m\omega^2 A^2 \sin^2\omega t\, dt + \int_0^T \frac{m\omega_0}{Q_{\text{cant}}} A^2\omega\cos\omega t\sin\omega t\, dt + \int_0^T kA^2\sin^2\omega t\, dt$$
$$-\int_0^T kA_{\text{drive}} A\cos\omega t\sin\omega t\, dt - \int_0^T k\Delta L A\sin\omega t\, dt$$
$$= \int_0^T F_{\text{ts}}(d + z(t))A\sin\omega t\, dt. \tag{17.2}$$

Since the integral of $\cos\omega t\sin\omega t$ over one period vanishes, the second and fourth terms on the left side in (17.2) vanish. The last term on the left side vanishes as well, since it is proportional to an integral of $\sin\omega t$ over one period. Thus (17.2) can be written as

$$(k - m\omega^2)A^2\int_0^T \sin^2\omega t\, dt = \int_0^T F_{\text{ts}}(d + z(t))A\sin\omega t\, dt. \tag{17.3}$$

The integral $\int\sin^2\omega t dt$ within the limits from 0 to T can be calculated as $\frac{1}{2}T = \frac{\pi}{\omega}$, which results in

$$(k - m\omega^2)A^2\frac{\pi}{\omega} = \int_0^T F_{\text{ts}}(d + A\sin\omega t)A\sin\omega t dt. \tag{17.4}$$

The left hand side of (17.4) can be further evaluated as follows

$$\frac{A^2\pi}{\omega}\left(k - m\omega^2\right) = \frac{A^2 m\pi}{\omega}\left(\frac{k}{m} - \omega^2\right)$$
$$= \frac{A^2 m\pi}{\omega}\left(\omega_0^2 - \omega^2\right) = \frac{A^2 m\pi}{\omega}\left(\omega_0 + \omega\right)\left(\omega_0 - \omega\right). \tag{17.5}$$

Since the tip-sample force is considered as a small perturbation, the frequency shift will be small as well, i.e. $\omega \approx \omega_0$ and $(\omega_0 + \omega) \approx 2\omega$. Thus, the left-hand side of (17.1) can be further written as

$$2\pi m A^2(\omega_0 - \omega) = -4\pi^2 m A^2(f - f_0) = -4\pi^2 m A^2\Delta f. \tag{17.6}$$

Now also taking the right-hand side of (17.4) into account the following expression for the frequency shift arises

$$\Delta f = -\frac{1}{4\pi^2 m A^2} \int_0^T F_{\mathrm{ts}}(d + A\sin\omega t) A \sin\omega t \; dt. \tag{17.7}$$

The time average of $F_{\mathrm{ts}}(t)$ times $z(t)$ over one period can be written as

$$\langle F_{\mathrm{ts}}(t) \cdot z(t) \rangle \equiv \frac{1}{T} \int_0^T F_{\mathrm{ts}}(d + A\sin\omega t) A \sin\omega t \; dt. \tag{17.8}$$

Using the above equation, (17.7) can be rewritten as the following expression for Δf (using $T = 1/f_0$ and $m = k/\omega_0^2$)

$$\Delta f = -\frac{f_0}{A^2 k} \langle F_{\mathrm{ts}}(t) \cdot z(t) \rangle. \tag{17.9}$$

The frequency shift is proportional to $\langle F \cdot z \rangle$, which is the time average of force times distance (tip-sample distance) over one oscillation period. The dependence as f_0/k on the resonance frequency and the spring constant is the same as in the small amplitude limit (14.8). In contrast to the case of small amplitudes, the frequency shift depends as $1/A^2$ on the oscillation amplitude.

As a consistency check we insert the force for a harmonic oscillator $F_{\mathrm{ts}} = -k'z$ as an approximation in the case of the small amplitude limit. This results in

$$\langle F_{\mathrm{ts}} \cdot z \rangle = -\langle k' \cdot z^2 \rangle = \frac{1}{T} \int_0^T -k' A^2 \cos^2 \omega t dt = -\frac{1}{2} k' A^2, \tag{17.10}$$

which recovers the result of the frequency change found for the small amplitude limit $\Delta f = f_0 k'/(2k)$ (cf. 14.8). In analogy to this result for the small amplitude limit an effective tip-sample spring constant can generally be defined as

$$k' \equiv -\frac{2\langle F_{\mathrm{ts}} \cdot z \rangle}{A^2}, \tag{17.11}$$

in order to recover an equation of the same form as in the small amplitude limit $\Delta f = f_0 k'/(2k)$.

17.1.1 Expression for the Frequency Shift

When analyzing the time average in (17.10) qualitatively, it can be seen that the parts of the oscillation path which make the largest contribution to the frequency change are the turnaround points. Here the velocity is lowest, so the tip stays longest at these positions (strongest contribution to the integral over time). The equilibrium position

is passed quickly at the largest velocity, leading to a small contribution to the time average. This dominant contribution of the turnaround points can be obtained more quantitatively if we replace the time average in (17.10) by a spatial average. A spatial average over the positions of the tip in one oscillation cycle is also more appropriate because the tip-sample force is primarily a function of tip-sample distance. For the average $\langle F \cdot z \rangle$ we wrote in (17.10)

$$\langle F_{\mathrm{ts}}(d+z) \cdot z \rangle = \frac{1}{T} \int_0^T F_{\mathrm{ts}}(d+z(t)) \cdot z(t) dt, \tag{17.12}$$

with $z(t) = A \sin \omega t$. In order to convert the time average to a spatial average over the trajectory, we substitute in (17.12) the variable t by z as

$$\frac{dz}{dt} = A\omega \cos(\omega t) = A\omega \sqrt{1 - \sin^2(\omega t)} = \omega \sqrt{A^2 - z^2}. \tag{17.13}$$

Therefore, the average $\langle F \cdot z \rangle$ can be written as

$$\begin{aligned} \langle F_{\mathrm{ts}}(d+z) \cdot z \rangle &= \frac{1}{T} \int_0^T F_{\mathrm{ts}}(d+z(t)) \cdot z(t) dt \\ &= \frac{2}{\omega T} \int_{-A}^{+A} \frac{F_{\mathrm{ts}}(d+z) \cdot z}{\sqrt{A^2 - z^2}} dz \\ &= \frac{1}{\pi} \int_{-A}^{+A} \frac{F_{\mathrm{ts}}(d+z) \cdot z}{\sqrt{A^2 - z^2}} dz. \end{aligned} \tag{17.14}$$

Combining (17.9) and (17.14) the following expression for the frequency shift is obtained

$$\Delta f = -\frac{f_0}{\pi k A^2} \int_{-A}^{+A} F_{\mathrm{ts}}(d+z) \frac{z}{\sqrt{A^2 - z^2}} dz = -\frac{f_0}{\pi k A^2} \int_{-A}^{+A} F_{\mathrm{ts}}(d+z) g(z) dz. \tag{17.15}$$

This can be interpreted as the integral of the tip-sample force from $-A$ to A with a weighting function $g(z)$. Due to this weighting function, the largest contributions to the frequency shift come from the regions close to the turnaround points of the oscillation $z = \pm A$. Here the weighting function diverges (denominator becomes zero) as seen in Fig. 17.2a. From the weighting function alone a large contribution to the frequency shift is expected at both turnaround points. However, the second factor in the integrand of (17.15), the tip-sample force F_{ts}, must also be considered.

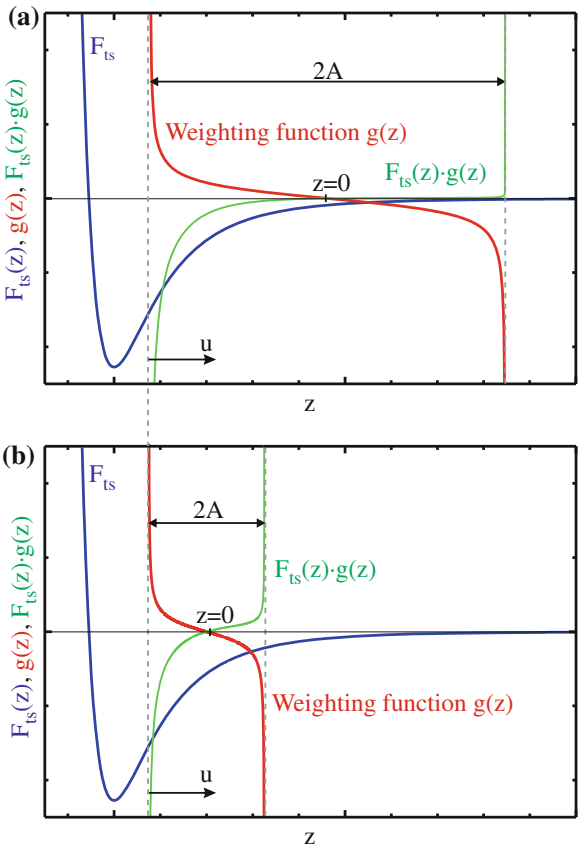

Fig. 17.2 The tip-sample force, the weighting function $g(z)$, and their product are displayed as a function of distance z for two different oscillation amplitudes A. In the large amplitude limit **a** the frequency shift signal is mainly picked up close to the lower turnaround point of the oscillation, while in the smaller amplitude case **b** contributions to the frequency shift are picked up during the whole oscillation cycle with the main contributions coming from both turnaround points. For better comparison, the lower turnaround point is kept constant in (**a**) and (**b**)

For the situation of a large amplitude shown in Fig. 17.2a the contribution to the frequency shift at the upper turnaround point $z = A$ is eliminated by the vanishing tip-sample force F_{ts}. The product of weighting function and tip-sample force, i.e. the integrand of (17.15) is shown as a green line in Fig. 17.2a. In total, for large amplitudes the contributions to the frequency shift come only from regions close to the lower turnaround point.

The case of a smaller oscillation amplitude is shown in Fig. 17.2b. For better comparability, the lower turnaround point of the oscillation was placed in the same position as in Fig. 17.2a. In this case, the integrand of (17.15) provides contributions to all parts of the oscillation cycle, since the force has appreciable values throughout the oscillation. The largest contributions to the frequency shift arise from both turnaround points, as shown by the green line in Fig. 17.2b.

Comparing the large amplitude case to the small amplitude case (Fig. 17.2a, b) we see that for the large amplitude case only the region close to the lower turnaround point contributes to the frequency shift, while the major part of the oscillation path does not result in a contribution to the frequency shift. In contrast, for small amplitudes

contributions to the frequency shift arise from all parts of the oscillation cycle. This means that for smaller oscillation amplitudes a stronger frequency shift signal is expected. In addition to this contribution from the integral in (17.15) also the prefactor $1/A^2$ enhances the frequency shift for small amplitudes. If we compare this amplitude dependence of the frequency shift, we note that in the previously treated small amplitude limit (14.8) the frequency shift was found to be independent of the oscillation amplitude. The strength of the signal is one issue, another is the corresponding noise, which also increases with decreasing amplitude, as will be discussed in Chap. 18. Together, the important figure of merit, the signal-to-noise ratio, will be obtained.

Due to the antisymmetric behavior of the weighting function with respect to the point of origin of the oscillation, a constant force will not lead to a frequency shift. This corresponds to the result obtained in the small amplitude limit that a constant force induces no frequency shift.

Often the total tip-sample force is considered as a superposition of different force contributions. Since the force enters linearly in (17.15) the total frequency shift can be split into contributions arising from the individual forces.

In this chapter, we have considered up to now conservative tip-sample interactions. In this case, the force is the same for a certain tip-sample distance independent of the direction of motion either for the approach towards the sample or for the retraction from the sample. For a dissipative tip sample interaction the forces at a certain point can be different for approach and retraction and this has to be considered. In this case, the tip-sample force in (17.15) can be replaced by $F_{\mathrm{ts}} = (F_{\mathrm{ts,approach}} + F_{\mathrm{ts,retraction}})/2$ [31, 32].

17.1.2 Normalized Frequency Shift in the Large Amplitude Limit

Up to now the coordinates have been chosen such that the reference for the position of the cantilever tip z was the equilibrium position of the cantilever (Fig. 17.1). This is the position in which the tip-sample force is compensated by the static bending force of the cantilever, also called the average tip position. In some cases, the lower turnaround point of the oscillation is a more useful reference point. Therefore, we now choose as a new distance variable $u = z + A$ in order to describe the tip position relative to the lower turnaround point (Fig. 17.1). If we substitute $z = u - A$ and express the tip-sample distance as $d + z = d - A + u$ the frequency shift (17.15) results in

$$\Delta f = -\frac{f_0}{\pi k A^2} \int_0^{2A} \frac{F_{\mathrm{ts}}(d - A + u)(u - A)}{\sqrt{A^2 - (u - A)^2}} du$$

$$= -\frac{f_0}{\pi k A^2} \int_0^{2A} \frac{F_{\mathrm{ts}}(d - A + u)(u - A)}{\sqrt{(2A - u)u}} du. \tag{17.16}$$

In the following, we consider the limit of a large oscillation amplitude, i.e. the oscillation amplitude A is much larger than the range of the tip-sample force. In this case the integrand in (17.15) or (17.16) has appreciable values only at tip positions very close to the lower turnaround point, as also indicated by the green line in Fig. 17.2a. The integrand $F_{\mathrm{ts}} \cdot g$ becomes negligible for larger values of u which, however, are still much smaller than A. Therefore, we take the limit $u \ll A$ and extend the integration limit to infinity, which results in

$$\Delta f = \frac{f_0}{\pi k A^2} \int_0^{\infty} \frac{F_{\mathrm{ts}}(d - A + u)A}{\sqrt{2Au}} du = \frac{f_0}{\sqrt{2}\pi k A^{3/2}} \int_0^{\infty} \frac{F_{\mathrm{ts}}(d - A + u)}{\sqrt{u}} du \ . \tag{17.17}$$

The dependences on resonance frequency and spring constant are the same as for the small amplitude limit (14.8). Furthermore, the frequency shift is proportional to $A^{-3/2}$.

The expression for the frequency shift in (17.17) contains two contributions. The frequency shift depends on the tip-sample force and also on the cantilever and experimental parameters. In order to separate the parameters out, a *normalized frequency shift* γ can be defined as

$$\gamma = \Delta f \frac{k A^{3/2}}{f_0} \ . \tag{17.18}$$

The normalized frequency shift has the following significance: Multiplying the experimentally measured frequency shift Δf by the factor $k A^{3/2}/f_0$, the expression (17.17) can be written as

$$\gamma = \frac{1}{\sqrt{2}\pi} \int_0^{\infty} \frac{F_{\mathrm{ts}}(d - A + u)}{\sqrt{u}} du \ . \tag{17.19}$$

The normalized frequency depends only on an integral over the tip-sample force, while the dependence on the experimental parameters k, f_0, and A is factored out.

The normalized frequency shift is particularly useful in order to compare experimental results obtained using different cantilevers (with different spring constants, and resonance frequencies) or results obtained using different oscillation amplitudes. The influence of all these parameters is factored out using the normalized frequency shift. In Fig. 17.3a measurements on a graphite sample are shown. The frequency shift is plotted as a function of tip-sample distance. Different frequency shift curves

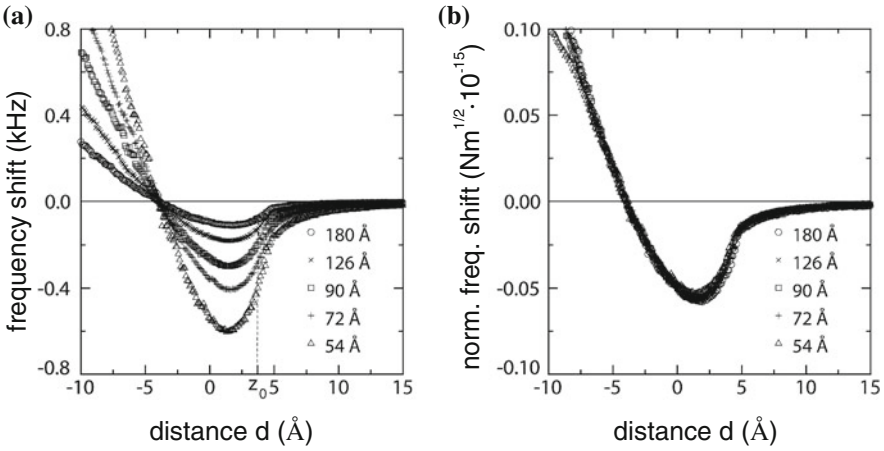

Fig. 17.3 **a** Experimentally measured frequency shift on a graphite sample as a function of the average tip-sample distance d for different values of the oscillation amplitude. The curves are shifted along the horizontal axis in order to make them comparable [33]. **b** If the normalized frequency shift is used as vertical axis, all curves for different amplitudes collapse to one curve, showing that the normalization has factored out the dependence on the amplitude (reproduced with permission from [33])

are obtained, for different oscillation amplitudes (always using the same cantilever). According to the previously obtained dependence, the measured frequency shift increases with decreasing oscillation amplitude. In Fig. 17.3b the normalized frequency shift is plotted, showing that all curves for different amplitudes collapse to one curve. This demonstrates the usefulness of the normalized frequency shift.

Now we evaluate the normalized frequency shift for a very simple model force which has a constant value of F_0 from the lower turnaround point up to a distance λ and is zero for larger distances. For this case, the normalized frequency shift can be evaluated using (17.19) as

$$\gamma = \frac{F_0}{\sqrt{2\pi}} \int_0^{\lambda} u^{-1/2} du = \frac{\sqrt{2}}{\pi} F_0 \sqrt{\lambda}. \tag{17.20}$$

To give some numbers: For $f_0 = 200\,\mathrm{kHz}$, $F_0 = 2\,\mathrm{nN}$, $A = 10\,\mathrm{nm}$, $k = 10\,\mathrm{N/m}$ and $\lambda = 0.1\,\mathrm{nm}$ a normalized frequency shift of $9\,\mathrm{fN}\sqrt{\mathrm{m}}$ results, corresponding to a frequency shift of $\Delta f = 180\,\mathrm{Hz}$. For an exponentially decaying force

$$F(z) = F_0 e^{-u/\lambda}, \tag{17.21}$$

the corresponding normalized frequency shift (17.19) can be calculated in the large amplitude limit as [34]

$$\gamma = \frac{1}{\sqrt{2\pi}} F_0 \sqrt{\lambda}, \tag{17.22}$$

which is (apart from a constant factor) the same result as obtained for a constant force F_0 with a range λ, shown in (17.20). Also for other forms of the tip-sample interaction, such as the Lennard-Jones interaction, the normalized frequency shift can be found in the literature [34].

17.1.3 Recovery of the Tip-Sample Force

In this chapter, we have derived equations of the (normalized) frequency shift for a given tip-sample force. Actually the reverse is desirable: It is desirable to recover the tip-sample force from the measured frequency shift. However, due to the integral present in (17.15) this equation cannot easily be inverted analytically to a solution for $F_{\mathrm{ts}}(\Delta f)$. In the small amplitude limit the obtained equation

$$\Delta f(d) = -\frac{f_0}{2k} \frac{\partial F_{\mathrm{ts}}(d+z)}{\partial z}\bigg|_{z=0}, \tag{17.23}$$

can be inverted to

$$F_{\mathrm{ts}}(d) = \frac{2k}{f_0} \int_d^\infty \Delta f(z')dz'. \tag{17.24}$$

The integration up to infinity shows that the frequency shift should be measured up to a position relatively far from the surface. For larger oscillation amplitudes, (17.15) can be inverted using approximations which allow the determination of the force with an accuracy of 5 % [32, 35].

17.2 Experimental Realization of the FM Detection Scheme

We have mentioned that in the FM detection mode the cantilever oscillation is always at resonance, i.e. it always follows the resonance frequency which changes under the influence of the tip-sample force. Now we will describe how this is achieved by the experimental setup. In this section, we introduce detection schemes which are used in the FM detection mode. Here it is not the amplitude change that is measured in response to a shift of the resonance frequency, but rather the shift of the resonance frequency itself is measured.

17.2.1 Self-excitation Mode

In the self-excitation mode the cantilever itself as a harmonic oscillator is the frequency-determining element in an oscillator circuit. A positive feedback is used

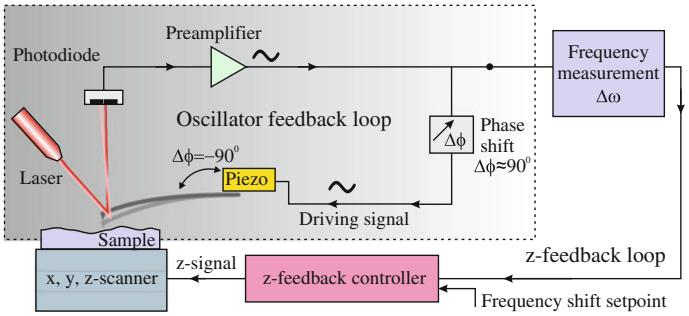

Fig. 17.4 Schematic of an FM detection setup operated in the self-excitation mode. In the circuit the measured cantilever oscillation signal is phase shifted and fed back to the actuator driving the cantilever. In addition to this (inner) oscillator feedback loop, the measurement of the shift of the resonance frequency $\Delta\omega$ is used in an outer z-feedback feedback loop in order to control the tip-sample distance

in order to self-excite the cantilever. A schematic of the implementation (Fig. 17.4) consists of an oscillator loop in which the measured oscillation signal is fed back (after a phase shift) as the driving signal of the cantilever. We will first discuss some essentials of this oscillator feedback loop and subsequently discuss its experimental realization. In addition to this oscillator feedback loop, the measured frequency shift of the resonance frequency $\Delta\omega$ is used in an outer z-feedback feedback loop in order to control the tip-sample distance.

In a mechanical harmonic oscillator oscillating at resonance there is a phase shift of $-90°$ between the displacement of the cantilever tip and the mechanical excitation, i.e. the cantilever oscillation is lagging the excitation. In the self-excitation scheme the measured cantilever oscillation signal is fed back as the excitation signal into the cantilever driving the piezo actuator (Fig. 17.4). In order to excite the cantilever with the correct resonance phase, a phase shift of $+90°$ has to be applied to the oscillation signal before feeding it back as the driving signal. This phase shift "compensates" the $-90°$ phase shift between mechanical excitation and oscillation of the cantilever. For simplicity, we neglect all other phase shifts present in the loop, for instance in the preamplifier. The detection of the cantilever deflection (by the photodiode and the preamplifier in the current example) is so fast that the deflection signal is sampled many times during one oscillation.

Since there is no external oscillator included driving the cantilever, the question arises as to how the cantilever oscillation is excited in the first place. The cantilever is *thermally* excited in a broad frequency range. Thermal excitation can be considered as white noise, i.e. having frequency components at all frequencies (cf. Chap. 18). If a frequency component of the thermal noise does not "hit" the resonance, the oscillation amplitude at this frequency will be small. The frequency component of the white noise which "hits" the resonance will be amplified Q times due to the resonance enhancement (transfer function) of a harmonic oscillator at the resonance frequency. Therefore, while uniformly excited over a wide frequency range by

thermal noise, a large oscillation amplitude occurs only at the resonance frequency. Due to this resonance enhancement the self-excitation mode self-excites its oscillation at the resonance frequency from thermal noise. This self-excitation works best for cantilevers with high quality factors. In the case of systems with low quality factors (like measurements in liquids), starting the self exciting oscillation is a problem. Also if the cantilever has multiple resonances, the self-excitation mode can be a bad choice. These problems are overcome in the PLL tracking mode of FM detection, which will be discussed in Sect. 17.2.3.

Another question is: Does the oscillation of the cantilever follow a change of the resonance frequency in the self-excitation mode? Let us assume an instantaneous change of the resonance frequency of the cantilever due to a change of the tip-sample interaction.[2] In the self-excitation mode, the cantilever is fed by its own oscillation. If the phase of the oscillator feedback loop is $-90°$, this means that the oscillator is automatically always fed at its resonance frequency. Due to this driving at resonance condition, the actual oscillation frequency will adapt to the new resonance frequency very fast.

This instantaneous adaption of the oscillation to the new resonance frequency can be demonstrated by including a term describing the self-oscillation loop in the equation of motion of the harmonic oscillator and subsequently solving this equation numerically. The self-excitation can be described in the equation of motion (2.17), replacing the driving term by the feedback term $\omega_0^2/Qz(t-t_0)$ [36]. The equation of motion for a harmonic oscillator with self-excitation then reads

$$\ddot{z} + \frac{\omega_0}{Q}\dot{z} + \omega_0^2 z = \frac{\omega_0^2}{Q} z(t-t_0). \tag{17.25}$$

The time shift $t - t_0$, with which the cantilever deflection signal is fed back as the driving signal $z(t - t_0)$, corresponds to a phase shift $\phi_0 = \omega t_0$, which is set to $-90°$. In order to demonstrate the tracking capability of the self-excitation mode, i.e. the fact that the actual cantilever oscillation frequency follows the change of the resonance frequency, the numerical solution of the equation of motion is analyzed. The response of the cantilever oscillation to an instantaneous change of the resonance frequency from ω_0 to ω_0' is simulated. Does the cantilever oscillation $z(t)$ follow the resonance frequency shift (tracking capability), and how rapidly is the new steady-state attained?

In Fig. 17.5 the deflection $z(t)$ obtained from the simulation is shown as a red line. The quick adaption of the oscillation to the new increased resonance frequency can be seen from the continuously increasing shift of the red curve relative to the reference curve (black line), corresponding to an oscillation without a change of the resonance frequency. In spite of the very large change of the resonance frequency of $\Delta\omega/\omega_0 = 5 \times 10^{-3}$, no transient occurs at $t = 0$. This is very different from

[2] For the case of AM detection, we have seen in Sect. 14.5 that after a change of the resonance frequency of the cantilever the new steady-state amplitude and phase are reached only after a large time constant $\tau_{\text{cant}} = 2Q/\omega_0$, corresponding to about Q oscillations.

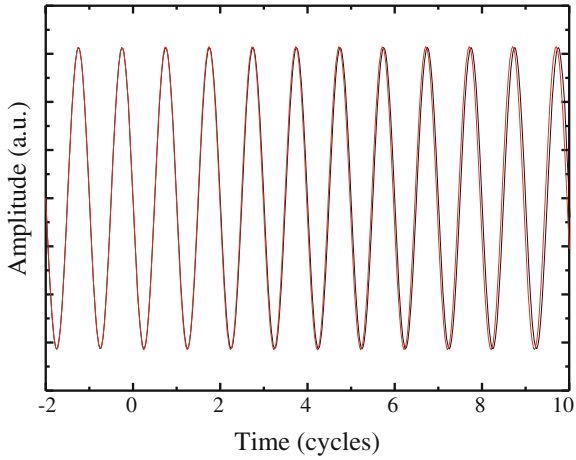

Fig. 17.5 Deflection $z(t)$ obtained from the simulation of a damped harmonic oscillator with self-excitation included in the equation of motion. At time $t = 0$ the resonance frequency of the harmonic oscillator changes from $f_0 = 1\,\text{MHz}$ by a large value of $\Delta f = 5\,\text{kHz}$. The simulated deflection (*red line*) is compared to the case without a change of the resonance frequency (*black line*). The fast adaption to the higher resonance frequency can be seen by a shift of the *red curve* with respect to the *black reference curve*. In spite of the large frequency shift assumed, the difference between the two *curves* is negligible at the time at which the resonance frequency changes ($t = 0$). This demonstrates the tracking capability of the self-oscillation mode with a very short time constant

AM detection, where a transient of about Q oscillation occurs before the oscillation has adapted to the new steady-state. The response of the cantilever oscillation to a change of the resonance frequency occurs instantaneously without a transient. After the change of the resonance frequency at $t = 0$ the amplitude remains constant. This is the case since the oscillation always remains in resonance. This is different from the AM case where the oscillation at ω_{drive} is off-resonance after a change of the resonance frequency. This leads to a reduced amplitude after a time constant of about Q oscillations in the AM mode, as seen in Fig. 14.8a.

The reason for the much shorter time constant in the self-excitation mode of the FM detection compared to the AM detection mode (cf. Sect. 14.5) can alternatively (to the analysis of the solution of the equation of motion) be rationalized by considering the change of the energy of the cantilever oscillation upon a change of the resonance frequency. The reason for the occurrence of the response time is that it takes time to transfer energy into, or remove energy from, the cantilever system during a transition to a new state with different amplitude/frequency. In the following, we will compare the energy change during this transition for the AM and FM modes. The energy difference between the free oscillator and the state with

tip-sample interaction present are compared for the two cases AM detection and FM detection.[3]

In the AM mode (e.g. tapping mode), a typical setpoint amplitude is 90 % of the free amplitude. The energy difference between the free oscillator and the oscillator with tip-sample interaction present results as

$$\Delta E_{\mathrm{AM}} = E_{\mathrm{free}} - E_{\mathrm{ts}} = \frac{1}{2} m\omega_0^2 A^2 - \frac{1}{2} m\omega_0^2 (0.9A)^2 = 0.19 E_{\mathrm{free}}. \tag{17.26}$$

In FM detection, the change of the energy occurs due to a change of the oscillation frequency, not the amplitude, which is kept constant in FM detection. A change of the resonance frequency from ω_0 to ω_0' leads to an energy change of

$$\begin{aligned} \Delta E_{\mathrm{FM}} &= E_{\mathrm{free}} - E_{\mathrm{ts}} = \frac{1}{2} m\omega_0^2 A^2 - \frac{1}{2} m\omega_0'^2 A^2 \\ &= \frac{1}{2} m\omega_0^2 A^2 \left(1 - \frac{\omega_0'^2}{\omega_0^2}\right) \approx E_{\mathrm{free}} \frac{2\Delta\omega}{\omega_0}. \end{aligned} \tag{17.27}$$

Typical values for the frequency shift in the FM detection mode are $\Delta\omega/\omega_0 = 10^{-4}$. Due to the small frequency shifts involved, the energy difference in FM mode is very small. According to (17.27) the energy change between the free cantilever and the cantilever under tip-sample interaction is $2 \times 10^{-4} E_{\mathrm{free}}$ in the FM mode, which is thousand times smaller than in the AM mode according to (17.26).

According to the definition of the Q-factor in (2.41), a damped harmonic oscillator can gain/lose roughly $1/Q$th of its energy in per cycle $E_{\mathrm{diss}} = 2\pi E_{\mathrm{osc}}/Q$. Thus for a Q factor of 10,000 an energy of $6 \times 10^{-4} E_{\mathrm{free}}$ can be dissipated per cycle, which is three times more than the energy change occurring in the FM mode. Hence the FM mode is not limited by slow response times for high Q-factors occurring for operation under vacuum conditions, as is the case for AM detection.

The fundamental reason for the slow response in AM detection is that a large energy change is required in order to change the amplitude, while in the FM detection scheme the energy change due to a change of the oscillation frequency of the sensor is much smaller, increasing the intrinsic bandwidth of the FM detection scheme. However, to detect a frequency shift of e.g. $\Delta\omega = 10^{-4}\omega_0$ and below will require a certain measurement (averaging) time which reduces the intrinsically high bandwidth.

After clarifying the fundamental issues i.e. phase shift of $+90°$ in order to maintain the resonance phase, self-excitation of the oscillator from thermal noise, and the tracking of the shifted resonance frequency, we now discuss the experimental realization of the outer z-feedback loop.

---

[3] This transition from the free state to the state with tip-sample interaction present (working point) gives an upper limit for energy changes occurring during scanning. Deviations from the setpoint values (amplitude/frequency shift) under feedback operation are much smaller than the deviations in amplitude/frequency shift between the free cantilever and the situation with tip-sample interaction present.

As discussed above, in the self-excitation mode the frequency of the cantilever oscillation automatically follows the resonance frequency of the cantilever. This frequency shift is measured by the frequency measurement unit in Fig. 17.4. We will go into the details of the frequency measurement later. For the moment let us assume that the frequency measurement unit delivers a voltage signal proportional to the frequency shift. This frequency shift signal is used as the feedback signal in order to control the tip-sample distance (z-feedback) in a second outer feedback loop. A fixed frequency shift is chosen as the setpoint and corresponds to a certain tip-sample distance. During an xy-scan a height contour of constant frequency shift is considered as the topography of the sample.

17.2.1.1 Amplitude Control and Dissipation

In FM detection, conservative and dissipative tip-sample interactions can be measured separately. The conservative part is measured via the measurement of the frequency shift, as discussed above. A dissipative tip-sample interaction leads to a reduction of the amplitude at resonance, but does not change the resonance frequency, as discussed in Fig. 14.9. Therefore, in FM detection the conservative tip-sample interaction and the dissipative tip-sample interaction can be separated by measuring the frequency shift on the one hand, and the amplitude change on the other hand. In the actual implementation, the oscillation amplitude is controlled to a fixed value by adjusting the excitation amplitude. If energy is dissipated by the tip-sample interaction the oscillation amplitude would decrease. However, an increased excitation amplitude will restore the desired (setpoint) oscillation amplitude. This amplitude-controlling part of the self-excitation scheme is included in the setup shown in Fig. 17.6.

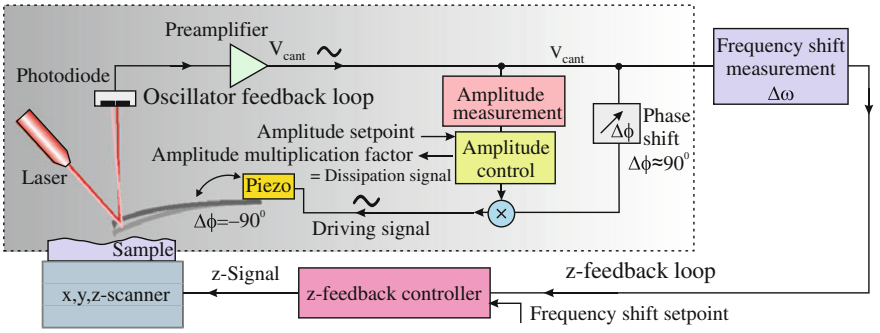

Fig. 17.6 Schematic of an FM detection setup operated with self-excitation including the amplitude control part. The cantilever oscillation amplitude is measured and maintained at a setpoint value by multiplying the driving signal by a proper multiplication factor. This factor relates to the energy dissipated by the tip-sample interaction

In order to maintain the oscillation amplitude at a certain setpoint value, the following scheme is applied. The amplitude of the cantilever oscillation signal is measured by an amplitude detection scheme (amplitude measurement block in Fig. 17.6). In a simple implementation an RMS-amplitude-to-DC converter can be used, in which the signal is rectified and low-pass filtered, resulting in a DC voltage proportional to the oscillation amplitude. The difference of this DC voltage to the amplitude setpoint value is taken as the error signal for an amplitude PI controller. The phase-shifted driving signal is multiplied by the appropriate amplitude factor obtained from the PI controller. In this way a constant cantilever oscillation amplitude is maintained by adjusting of the amplitude of the driving signal.

The amplitude multiplication factor in the amplitude control depends on the tip-sample dissipation energy as follows. If energy is lost by an increasing tip-sample dissipation, the oscillation amplitude decreases. This is detected by the amplitude detection unit and compared to the desired amplitude setpoint. The output of the amplitude control unit (PI controller) is a multiplication factor by which the driving signal is multiplied in order to generate a constant cantilever oscillation amplitude. Therefore, this amplitude multiplication voltage can also serve as an output signal related to the dissipation. This dissipation signal can be recorded as a free signal during a scan. The relation between the oscillation amplitude and the energy dissipated by the tip-sample interaction is given by (15.18).

The 90° phase shift applied in the feedback circuit in order to drive the cantilever at resonance is an idealization. In practice additional phase shifts of other components (preamplifier) in the circuit have to be compensated. The phase shift in the box called the phase shift in Fig. 17.6 is adjusted (deviating from 90°) in such a way that a minimum driving amplitude is required in order to establish a certain oscillation amplitude of the cantilever (resonance condition).

To summarize, in the self-excitation mode the oscillation signal is fed back as the driving signal with a 90° phase shift. This sustains an oscillation which always follows the resonance frequency of the cantilever quasi instantaneously. The following actual measurement of this frequency will be discussed next. The amplitude multiplication factor applied to the measured oscillation signal provides information about the dissipation of the tip-sample interaction. Due to amplitude control, the cantilever oscillates at a constant amplitude. With high quality factor sensors, the oscillation will start by itself excited by thermal noise.

17.2.2 Frequency Detection with a Phase-Locked Loop (PLL)

There are several ways to measure a frequency (shift). In FM AFM the phase-locked loop detection (PLL) method is used often for this purpose, because with this method frequency shifts can be measured with high accuracy in a wide frequency range. As a starting point, we demonstrate that a change of the frequency of an oscillation can be alternatively expressed as a time-dependent phase. If the frequency of an oscillation is ω, the oscillation can be written as $\cos(\omega t + \phi_0)$. If the oscillation frequency changes

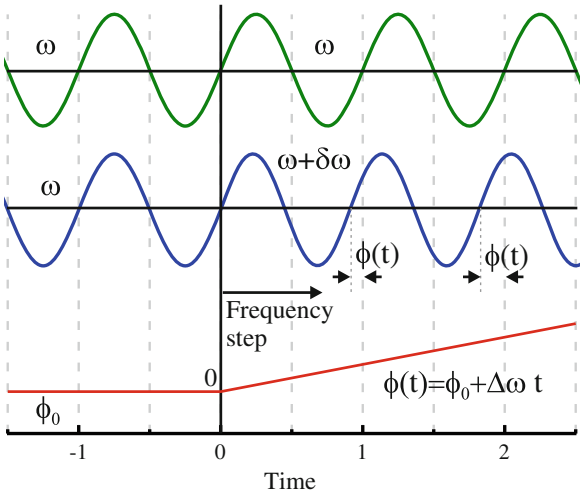

Fig. 17.7 The slightest frequency increase from ω to $\omega + \delta\omega$ leads to a linearly increasing phase $\phi(t)$. This phase (difference) can be detected using a phase detector. If the phase difference is maintained at zero, the two frequencies are exactly the same

at $t = 0$ form ω to $\omega + \delta\omega$, the oscillation can be expressed as $\cos[(\omega + \delta\omega)\, t + \phi_0]$. However, alternatively this expression can be rewritten as

$$\cos[(\omega + \delta\omega)\, t + \phi_0] = \cos[\omega t + (\delta\omega t + \phi_0)] = \cos(\omega t + \phi(t))\,, \qquad (17.28)$$

with $\phi(t) = \delta\omega t + \phi_0$. Thus a frequency change can also be expressed as a time-dependent phase $\phi(t)$ which increases linearly with time, as shown in Fig. 17.7. The slightest frequency change corresponds to a linearly increasing phase signal. If the phase $\phi(t)$ is zero (or generally constant), the two frequencies are exactly the same.

In the following, the inner working of the frequency shift measurement (box in Fig. 17.6) will be explained for the case that a PLL is used for the frequency measurement. In a PLL the frequency of an internal oscillator is controlled to match (follow) the frequency of the cantilever oscillation.

A PLL used in AFM is shown in Fig. 17.8 and consists of three main components: a phase detector, a Voltage-Controlled Oscillator (VCO), and a controller. First we introduce the phase detector and the VCO. Subsequently, their interaction in a phase-locked loop is described.

In the phase detector, the phase of the cantilever oscillation signal $V_{\text{cant}} \propto \cos(\omega_{\text{cant}} t)$ is compared to the phase of the signal from the voltage-controlled oscillator $V_{\text{vco}} \propto \cos(\omega_{\text{vco}} t + \phi_0)$ and the relative phase $\phi(t)$ is detected. In the phase detector, the two signals are multiplied and due to a mathematical identity the product can be written as

$$V_{\text{cant}} \cdot V_{\text{vco}} \propto \frac{1}{2}\left(\cos[(\omega_{\text{cant}} + \omega_{\text{vco}})t + \phi_0] + \cos[(\omega_{\text{vco}} - \omega_{\text{cant}})t + \phi_0]\right). \qquad (17.29)$$

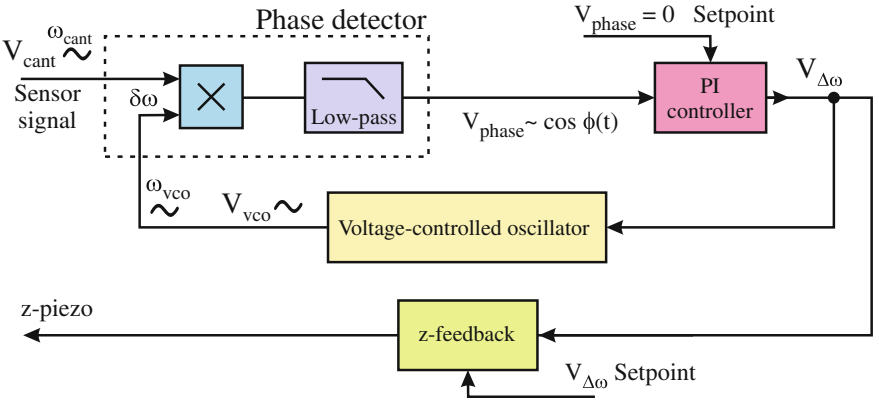

Fig. 17.8 The phase-locked loop consists of three main components: a phase detector, a Voltage-Controlled Oscillator (VCO) and a controller. These are combined to form a feedback loop in which the phase detector detects the phase difference between the cantilever oscillation signal V_{cant} and the VCO signal V_{vco}. The controller regulates the VCO frequency to a vanishing V_{phase}. This means that the VCO frequency adapts the cantilever frequency $\omega_{\text{vco}} = \omega_{\text{cant}}$ and the phase between the cantilever oscillation and the VCO signal is $\phi_0 = 90°$. Thus the frequency of the VCO follows the cantilever oscillation frequency and a voltage proportional to the frequency shift $V_{\Delta\omega}$ is obtained at the output of the controller

The low-pass filter in the phase detector removes the component with the sum of the frequencies. Thus the signal at the output of the phase detector results as

$$V_{\text{phase}} \propto \cos\left[(\omega_{\text{vco}} - \omega_{\text{cant}})t + \phi_0\right] = \cos(\delta\omega t + \phi_0) = \cos(\phi(t)), \qquad (17.30)$$

with $\delta\omega = \omega_{\text{vco}} - \omega_{\text{cant}}$. The measured phase signal V_{phase} has the largest phase sensitivity for a phase close to 90°. Therefore, we consider $V_{\text{phase}} = 0$ as the working point, corresponding to $\phi_0 = 90°$. Relative to this working point, the cosine function has a slope of minus one and the phase signal can be approximated (for small $\delta\omega t$) as $V_{\text{phase}} \propto -\delta\omega t$. Including a proportionality factor K_{pd} which converts the phase into a voltage, the output voltage of the phase detector can be written as

$$V_{\text{phase}} = K_{\text{pd}} \cos\left(\delta\omega t + 90°\right) \approx -K_{\text{pd}}\delta\omega t. \qquad (17.31)$$

We do not consider the inner working of the voltage-controlled oscillator (VCO) here. For us the VCO is just a block in which the input voltage $V_{\Delta\omega}$ controls the output frequency linearly relative to the working frequency as

$$\omega_{\text{vco}} = \omega_{\text{work}} + K_{\text{vco}} V_{\Delta\omega}, \qquad (17.32)$$

with the proportionality factor K_{vco}, converting the input voltage $V_{\Delta\omega}$ to a frequency shift relative to the working frequency. The working frequency is the frequency of the free cantilever plus the frequency shift setpoint $\omega_{\text{work}} = \omega_{\text{free}} + \Delta\omega_{\text{set}}$.

Now we discuss the frequency tracking capability of the PLL. For the moment, we do not consider the PI controller shown in Fig. 17.8 and assume that the phase signal V_{phase} is directly fed into the input of the VCO, i.e. $V_{\text{phase}} = V_{\Delta\omega}$. Let us assume that initially the frequency of the VCO matches the oscillation frequency of the cantilever, $\omega_{\text{vco}} = \omega_{\text{cant}} = \omega_{\text{work}}$ and $\phi_0 = 90°$. At this working point $V_{\text{phase}} = 0$, which corresponds to the condition of maximum sensitivity for the phase, as shown above. In this case the input voltage at the VCO vanishes, i.e. $V_{\Delta\omega} = 0$.

Now we consider a change of the actual oscillation frequency of the cantilever, which results in a frequency difference $\delta\omega$ between the cantilever oscillation frequency and the VCO frequency. According to (17.31) this frequency difference leads to a phase difference signal measured by the phase detector $V_{\text{phase}} = K_{\text{pd}} \cos(\delta\omega t + \phi_0)$, which evolves approximately linearly with time. With this input, the output frequency of the VCO results according to (17.32) as

$$\omega_{\text{vco}} = \omega_{\text{work}} + K_{\text{pd}} K_{\text{vco}} \cos(\delta\omega t + \phi_0) \,. \tag{17.33}$$

Directly after the instantaneous frequency shift by $\Delta\omega$, the relations $\delta\omega = \Delta\omega$ and $\phi_0 = 90°$ hold. According to (17.33), the linearly increasing phase $\delta\omega t$ leads to an increasing ω_{vco}. This reduces the frequency difference $\delta\omega$ between the cantilever frequency and the frequency of the VCO, i.e. $\delta\omega < \Delta\omega$. Any remaining finite frequency mismatch $\delta\omega$ leads over time to an increasing phase $\delta\omega t$ bringing the VCO frequency closer to ω_{cant}. In this way, the VCO frequency adapts to the (changed) frequency of the cantilever $\omega_{\text{work}} + \Delta\omega$. Due to this mechanism the VCO frequency is said to be locked to the cantilever frequency. In the steady-state $\omega_{\text{vco}} = \omega_{\text{cant}}$ and the frequency mismatch $\delta\omega = 0$ vanishes.[4]

In the terminology of the PLL: The VCO frequency is *locked* to the cantilever oscillation frequency by a *phase* comparison of both signals in a feedback *loop*. Hence, the name *phase-locked loop*. In this way, the PLL measures the frequency of the AFM sensor as the voltage $V_{\Delta\omega}$. This voltage, which is proportional to the frequency shift $\Delta\omega$, is used in the z-feedback loop to control the tip-sample distance. A certain tip-sample distance corresponds to a certain frequency shift voltage $V_{\Delta\omega}$, which is kept constant by the z-feedback loop (Fig. 17.6).

The original cantilever signal is a high-frequency signal close to ω_0, which is modulated to slightly lower or higher frequencies (at a much lower frequency) by the tip-sample interaction, for instance during scanning of an atomic corrugation (without z-feedback). The PLL converts this modulated high frequency signal to a

[4] While the PLL provides a frequency match $\omega_{\text{vco}} = \omega_{\text{cant}}$, a phase $\phi_0 \neq 0$ remains. The relation

$$\omega_{\text{cant}} = \omega_{\text{work}} + \Delta\omega \stackrel{!}{=} \omega_{\text{vco}} = \omega_{\text{work}} + K_{\text{pd}} K_{\text{vco}} \cos(\delta\omega t + \phi_0) \,, \tag{17.34}$$

results for the condition $\delta\omega = 0$ in

$$\Delta\omega = K_{\text{pd}} K_{\text{vco}} \cos\phi_0 . \tag{17.35}$$

Thus a static phase difference ϕ_0 different from $\phi_0 = 90°$ evolves in order to adapt the VCO frequency to the changed cantilever frequency.

low frequency signal proportional to the frequency modulation of the high frequency signal. This is called FM demodulation and also occurs in an FM radio receiver, where a high-frequency carrier signal is modulated by a low-frequency audio signal and the demodulation of the audio signal is desired.

Without the use of the PI controller (not yet applied) the frequency match of the VCO frequency is achieved by a phase ϕ_0 different from 90°, as shown in (17.35). Thus the desired working point at $\phi_0 = 90°$ is left. In order to enforce a vanishing phase signal (i.e. to maintain the condition $\phi_0 = 90°$) a PI controller is used, which controls V_{phase} to zero by generating an appropriate controller output signal $V_{\Delta\omega}$, which is used as the input voltage for the voltage-controlled oscillator.

17.2.3 PLL Tracking Mode

We have considered the cantilever as an ideal harmonic oscillator. Due to the non-ideal properties of the mechanical cantilever oscillator, the cantilever oscillation can deviate from the ideal sinusoidal shape. Moreover, a cantilever is a 3D object that has many modes which can sometimes be located at frequencies close to each other. An excitation of modes close to the desired resonance frequency can also lead to deviations from a clean sinusoidal oscillation. In order to feed the cantilever with a very clean sinusoidal signal the PLL tracking mode is often used instead of the self-excitation mode.

In the PLL tracking mode, the signal at the output of the VCO, which has a very clean sine shape, is used to excite the cantilever (Fig. 17.9). The cantilever deflection signal (sensor signal) is fed to the input of the PLL (we neglect the amplitude control for the moment).

In the following, we analyze the time constants of the PLL tracking mode and obtain the result that this mode has a larger time constant than the self-excitation mode. We consider an instantaneous jump of the cantilever resonance frequency due to a tip-sample interaction from ω_0 to ω_0'. Initially after this jump the excitation frequency (PLL output) still remains at ω_0. This corresponds to the situation in the AM detection mode: excitation at a fixed frequency ω_0 and instantaneous change of the cantilever resonance frequency. For the case of AM detection, we found in Sect. 14.5 that the amplitude and now more importantly the phase changes with a time constant of $\tau_{\text{cant}} = 2Q/\omega_0$. The PLL detects this slowly changing phase and adapts the VCO frequency with the time constant τ_{cant} to the cantilever frequency.[5] Thus

[5] This is the case for a PLL with a fast time constant. If the PLL has a time constant longer than τ_{cant}, the PLL time constant will limit the overall time constant.

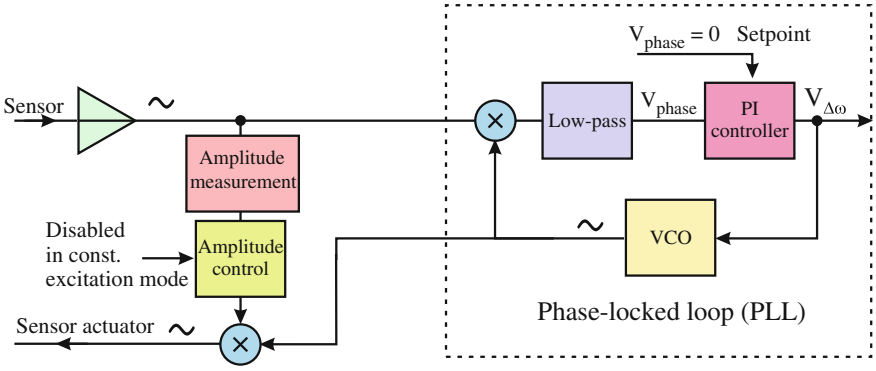

Fig. 17.9 Schematic of an FM AFM control in the PLL tracking mode. In this mode, the sensor is excited by a very clean sinusoidal driving signal taken from the voltage-controlled oscillator (VCO)

the PLL tracking mode is, compared to the self-excitation mode, a slow detection mode. As an example, for a Q-factor of 10^4 and $f_0 = 150\,\text{kHz}$ a time constant $\tau_{\text{cant}} = 130\,\text{ms}$ results.

Another disadvantage in using the excitation signal from the PLL is the following. If the PLL becomes unlocked, the cantilever will no longer be excited at its resonance and the z-feedback will not work properly anymore. In the self-excitation scheme the cantilever always oscillates at its resonance frequency independent of the PLL frequency detection.

The PI controller in the PLL loop (Fig. 17.9) is of specific importance if the VCO excites a harmonic oscillator (the cantilever) at resonance, as is the case in the PLL tracking mode.[6] Without the PI controller, according to (17.35), any deviation from the working frequency $\Delta\omega$ leads to a constant phase shift ϕ_0 different from 90°. This means that the cantilever is excited with a phase deviating from the proper resonance phase 90°. Specifically for cantilevers with high Q-factors, even a small phase shift leads to a driving out of resonance. The desired driving of the cantilever at resonance can be maintained by the use of a PI controller. Using the PI controller in the PLL loop, the phase signal ($V_{\text{phase}} = \cos(\delta\omega t + \phi_0)$) is kept at zero by delivering a proper $V_{\Delta\omega}$ signal. Thus with a PI controller both the phase shift of $\phi_0 = 90°$ (driving the cantilever at resonance) as well as tracking the VCO frequency to the cantilever frequency ($\delta\omega = 0$) are maintained.

The oscillation amplitude control is usually implemented in the same way as in the self-excitation mode. In a variant of the PLL tracking mode the oscillation amplitude is not kept at a constant value, but the sensor excitation amplitude is set to a fixed value. This mode is called constant excitation mode.

[6] In the PLL circuits used for example in communications, the PI controller is often not included.

17.3 The Non-monotonous Frequency Shift in AFM

FM detection can be operated both in the attractive and also in the repulsive regime of the tip-sample force. This advantage also involves a disadvantage. The measured property, the frequency (shift), depends non-monotonously on the tip-sample distance, as can be seen in Fig. 17.3a and schematically in Fig. 17.10a. Due to this, the tip-sample distance can only be controlled in a certain range of distances. As shown in the following, instabilities occur outside of this range.

In STM the measured signal (tunneling current) increases monotonously (exponentially) with decreasing tip-sample distance. This leads to stable feedback, i.e. the feedback controller "knows what to do". If the current becomes larger (e.g. due to

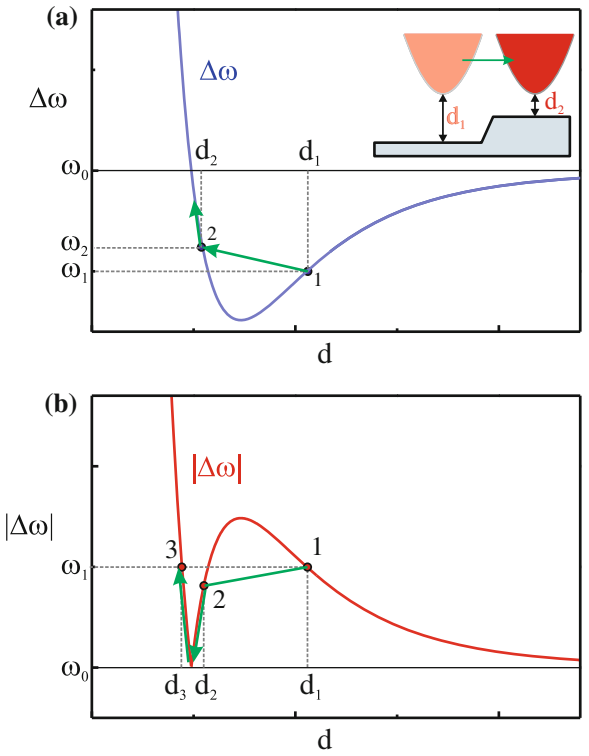

Fig. 17.10 Instabilities arise due to the non-monotonous dependence of the measured frequency shift as a function of the tip-sample distance. **a** An instability in the attractive regime at working point d_1 (induced for instance due to a fast scan over a steep step edge (inset)) results at a new working point at d_2 with opposite slope, leading to a wrong direction of the feedback action and to a crash of the tip into the surface. **b** Catastrophic events can be prevented by using the absolute value of the frequency shift as the signal for the feedback. In this case, the working point at d_1 is lost if the tip-sample distance changes suddenly to d_2, but instead of a catastrophic tip crash a stable working point in the repulsive branch at d_3 is reached

moving over a step edge), the tip has to be withdrawn from the sample in order to recover the desired tip-sample distance. A severe problem arises if the measured signal changes in a *non-monotonous* way with the tip-sample distance.

Let us assume that stable feedback is established at the tip-sample distance d_1 in the attractive regime at the frequency setpoint ω_1 (point 1 in Fig. 17.10a). Here the frequency shift $\Delta\omega(d)$ has a positive slope. Due to some event, like a steep step edge, the tip-sample distance can potentially decrease suddenly to d_2, corresponding to a frequency ω_2. The feedback would now try to restore the setpoint frequency (shift) ω_1. However, due to the opposite slope of the frequency shift at point 2, the feedback moves the tip closer and closer to the surface. The feedback "thinks" the tip has to be moved towards the sample in order to restore the more negative frequency shift ω_1. This will lead to a catastrophic event (positive feedback) in which the tip crashes into the sample up to the maximum range the piezo element can extend. The change from one branch of the frequency shift curve to that of the opposite slope can occur for various reasons: a steep slope in the surface topography, a protrusion on the surface, noise in the measurement signal and lateral change of the interaction potential (i.e. a branch of opposite slope is reached for a different lateral tip position on the sample).

Stable feedback can be provided only for a range in which the measured signal monotonously increases (decreases) with the tip-sample distance. One way to improve the situation is not to use the frequency shift, but the *absolute value* of the frequency shift $\Delta\omega$ as the feedback signal, as shown in Fig. 17.10b. If here the working point at d_1 is left, also an instability occurs in the region of opposite (positive) slope, for instance at point 2. However, in this case no catastrophic event occurs since the tip approaches the surface only until stable feedback is resumed in the branch with a negative slope and an unintended stable working point 3 is reached. Thus, using the absolute value of the frequency shift signal avoids catastrophic tip crashes and stabilizes the feedback (in the case of an instability) in the repulsive regime. However, the intended working point in the attractive regime is replaced by a working point in the repulsive regime.

Another way to cope with this non-monotonous frequency shift is to work in the constant height mode. In this case no instability will occur, since the feedback is off. However, the constant height mode can be operated only for very flat surfaces and under very stable conditions where drift does not change the height, i.e. at low temperatures.

17.4 Comparison of Different AFM Modes

In the previous chapters, we have discussed several modes of AFM operation, which we will now compare. In Table 17.1 operating modes are sorted along two coordinates: the operating mode can be static or dynamic and the interaction regime can be attractive or net-repulsive. Often the static AFM is taken to be synonymous with contact AFM (net repulsive interaction), while dynamic AFM is taken to be synonymous

Table 17.1 Operating modes of AFM ordered in two "coordinates": static/dynamic mode and attractive/net-repulsive interactions

	Static AFM	Dynamic AFM
Net-repulsive interaction Contact	Contact mode: k ∼ 1 N/m	Tapping mode: k ∼ 20–100 N/m
Attractive interaction Non-contact	Non-contact mode: k ∼1 N/m	AM/FM non-contact mode: k ∼ 20–10^6 N/m

with non-contact AFM (attractive interaction). However, also the off-diagonal elements in Table 17.1 are possible.

The static AFM is usually operated with tip and sample in contact (snap-to-contact), which corresponds to the upper left entry in the table. However, the static detection method can also be used in the regime of attractive interaction (non-contact). For instance, long-range electric or magnetic forces can be measured using static AFM in the non-contact mode (lower left off-diagonal element in the table). In this mode possible instabilities can lead to snap-to-contact.

In the dynamic modes, snap-to-contact is avoided and the contact/non-contact "coordinate" has to be assigned differently. The contact regime can be assigned to the range where a net repulsive force acts between the tip and sample, while in non-contact the force between tip and sample is attractive.

In the dynamic modes, we measure changes in the vibrational properties of the cantilever due to tip-sample interactions. The measured properties include the resonance frequency, the oscillation amplitude, and the phase between excitation and oscillation of the cantilever. The dynamic AFM can either operate in the non-contact mode (lower right entry in the table) or in the intermittent contact mode (tapping mode) where a repulsive tip-sample contact is established at the lower turnaround point of the oscillation (upper right off-diagonal entry in the table). In dynamic mode, snap-to-contact has to be avoided because no oscillation can be sustained. Therefore, cantilevers used in the dynamic mode have a higher force constant than cantilevers used in contact mode, or alternatively the amplitudes used are large.

17.5 Summary

- In the FM detection scheme the oscillation frequency follows the shift of the resonance frequency, i.e. the cantilever always oscillates at resonance.
- The frequency shift in the FM detection is given as

$$\Delta f = -\frac{f_0}{A^2 k}\langle F_{\mathrm{ts}}(t)\cdot z(t)\rangle = -\frac{f_0}{\pi k A^2}\int_{-A}^{+A} F_{\mathrm{ts}}(d+z)\frac{z}{\sqrt{A^2-z^2}}dz. \quad (17.36)$$

- In the large amplitude limit (amplitude much larger than the range of the tip-sample force) the normalized frequency shift γ factors the dependence on the experimental parameters out and is given by

$$\gamma = \Delta f \frac{kA^{3/2}}{f_0} \,. \tag{17.37}$$

  Thus the normalized frequency shift depends only on an integral over the tip sample force.
- In the self-excitation scheme the cantilever is self-excited from thermal noise at the momentary resonance frequency of the cantilever. The cantilever oscillation signal is measured and fed back (after an appropriate phase shift) as the cantilever driving signal.
- If in FM detection the amplitude is kept at a constant value (amplitude control), the corresponding multiplication factor contains information about the tip sample dissipation.
- In the FM mode the frequency of the cantilever oscillation is usually measured by a phase-locked loop (PLL). The measured frequency shift signal is used to control the tip-sample distance via a z-feedback loop.
- In the PLL tracking mode the cantilever driving signal is taken from an oscillator of the PLL. This has the advantage of driving the cantilever with a very clean sinusoidal signal.
- The non-monotonous dependence of the frequency shift on the tip-sample distance can lead to instabilities. These can be prevented by taking the absolute value of the measured frequency shift as the signal for the z-feedback.
- The response time to adapt the steady-state oscillation signal after an instantaneous change of the tip-sample interaction is much shorter in the case of FM detection than for AM detection. Therefore, the FM detection scheme is used for the case of high Q-factors, i.e. in vacuum.
- The AFM modes can be ordered in two coordinates: static/dynamic and net repulsive (contact)/attractive (non-contact). The static AFM in the net repulsive regime is termed the contact mode and the dynamic mode in the attractive regime is called the non-contact mode. However, besides these regimes, the static mode can also be operated in the attractive interaction regime, and the dynamic mode can be operated in the net repulsive interaction regime (intermittent contact).